

X-ray magnetic circular dichroism probe of the Rh magnetic moment instability in $\text{Fe}_{1-x}\text{Rh}_x$ alloys near the equiatomic concentration

Jesús Chaboy, Fernando Bartolomé, M. R. Ibarra, C. I. Marquina, and P. A. Algarabel

Instituto de Ciencia de Materiales de Aragón and Departamento de Física de la Materia Condensada, Consejo Superior de Investigaciones Científicas, Universidad de Zaragoza, 50009 Zaragoza, Spain

Andrei Rogalev and Claus Neumman

European Synchrotron Radiation Facility, Boîte Postale 220, 38042 Grenoble Cedex, France

(Received 4 September 1998)

X-ray magnetic circular dichroism (XMCD) measurements performed at the Rh $L_{2,3}$ edges and Pd L_3 edge in $\text{Fe}_{0.51}\text{Rh}_{0.49}$ and $\text{Fe}_{1.005}(\text{Rh}_{0.85}\text{Pd}_{0.15})_{0.995}$ evidence the instability of the Rh magnetic moment (μ_{Rh}) through the ferromagnetic-antiferromagnetic transition and demonstrate the induced nature of both μ_{Rh} and μ_{Pd} . In the case of $\text{Fe}_{0.51}\text{Rh}_{0.49}$ these experiments have also revealed the existence of a ferromagnetic ground state at low temperatures in which $\mu_{Rh} \sim 0.7\mu_B$. [S0163-1829(99)11605-9]

The peculiar magnetic properties of the Fe-Rh alloys near the equiatomic composition have fascinated a lot of scientists for over 50 years, so that since the pioneer works of Fallot and Hocart,¹ a large number of experimental and theoretical studies have been published.²⁻⁴ Equiatomic FeRh undergoes a first-order transition from paramagnetic (PM) to ferromagnetic (F) state at $T_c \sim 650$ K, and a peculiar ferromagnetic-antiferromagnetic phase transition at about $T_{F-AF} = 350$ K. Both T_c and T_{F-AF} transition temperatures are very sensitive to composition, being the F-AF transition only present in a very narrow concentration range of about 5% around $x = 0.5$ in the binary $\text{Fe}_{1-x}\text{Rh}_x$ phase diagram, and the ground state becoming ferromagnetic for $x = 0.51$.^{5,6}

The magnetic structure of both F and AF phases has been determined by means of neutron diffraction and Mössbauer experiments: in the F phase the Fe and Rh moments are parallel and ferromagnetically ordered, while in the AF phase only the Fe atoms carry magnetic moment. Bertaut and co-workers reported $\mu_{Fe} = 3.04\mu_B$ and $\mu_{Rh} = 0.62\mu_B$ for the 53% Rh alloy at 330 K and $\mu_{Fe} = 2.84\mu_B$ and $\mu_{Rh} = 0.8\mu_B$ at 373 K, where the alloy is ferromagnetic, and $\mu_{Fe} = 3.3\mu_B$ in the AF phase at room temperature.^{7,8} On the other hand, Shirane and co-workers reported for a single crystal of the 48% Rh alloy, ferromagnetic at room temperature, that the atomic moments are $\mu_{Fe} = 3.2\mu_B$ and $\mu_{Rh} = 0.9\mu_B$.⁹

The magnetic structure of the AF phase was a matter of discussion as far as the rhodium moment is concerned. Only Shirane and co-workers attempted a determination of the Rh moment in the AF phase and came to the conclusion that if such a moment existed, it was less than its value of $1\mu_B$ found in the F phase. Recent first-principle band structure calculations have predicted the coexistence of AF and F phases over a wide range of volume.² The zero pressure equilibrium state is found to be AF with $\mu_{Fe} \sim 3\mu_B$ and zero μ_{Rh} , and the metastable F state can be reached either thermally or by applying a magnetic field.

Consequently, so far there is no direct evidence for the existence of a finite moment at the rhodium site, the general opinion widely accepts that $\mu_{Rh} = 0$ in the AF phase, and that

both Fe and Rh moments are parallel and ferromagnetically ordered in the F phase, not only regarding FeRh alloys but also their substitutional derivatives. However, this commonly accepted picture is mainly based upon the work of Bertaut and co-workers and Shirane *et al.* performed in the early sixties.⁷⁻⁹ To our knowledge, no other results have been published regarding both the coupling and magnitude of Fe and Rh moments, as well as no information has been gained regarding the sign and magnitude of the moments on the substitutional atoms.

In this work we report x-ray magnetic circular dichroism (XMCD) measurements performed at the Rh $L_{2,3}$ edges and Pd L_3 edge in $\text{Fe}_{0.51}\text{Rh}_{0.49}$ and $\text{Fe}_{1.005}(\text{Rh}_{0.85}\text{Pd}_{0.15})_{0.995}$ compounds. In the case of the Fe-Rh-Pd sample, which exhibits the characteristic F-AF transition similar to that found in equiatomic FeRh, the aim of the XMCD study is to get an insight about both the magnitude and nature of the magnetic moment on both Rh and Pd atoms. The ferromagnetic $\text{Fe}_{0.51}\text{Rh}_{0.49}$ system has been studied in order to investigate the possible existence of a μ_{Rh} thermal instability as the origin for the large magnetovolumic effect observed in this system below $T = 150$ K.³

Polycrystalline $\text{Fe}_{0.51}\text{Rh}_{0.49}$ and $\text{Fe}_{1.005}(\text{Rh}_{0.85}\text{Pd}_{0.15})_{0.995}$ samples were used for the experiments. Details of samples preparation and characterization can be found in Refs. 3 and 10. The description of the experimental setup used for the magnetization, thermal expansion and magnetostriction measurements can be also found in Ref. 3. The XMCD experiments at the Rh $L_{2,3}$ edges were carried out at the ESRF beamline 6 (ID12A) which is dedicated to polarization dependent x-ray-absorption studies.¹¹ The source is the helical undulator HELIOS II which emits x-ray radiation with a high polarization rate of above 97% and flexible polarization (circular left-circular right). The first harmonic of the undulator spectrum was selected to cover the range from 2.9 to 3.2 keV, i.e., Rh $L_{2,3}$ and Pd L_3 edges were tuned. The fixed-exit double-crystal monochromator was equipped with a pair of Si(111) crystals cooled down to -140°C . In this configuration the Bragg angle is close to 45° giving rise to the drop of

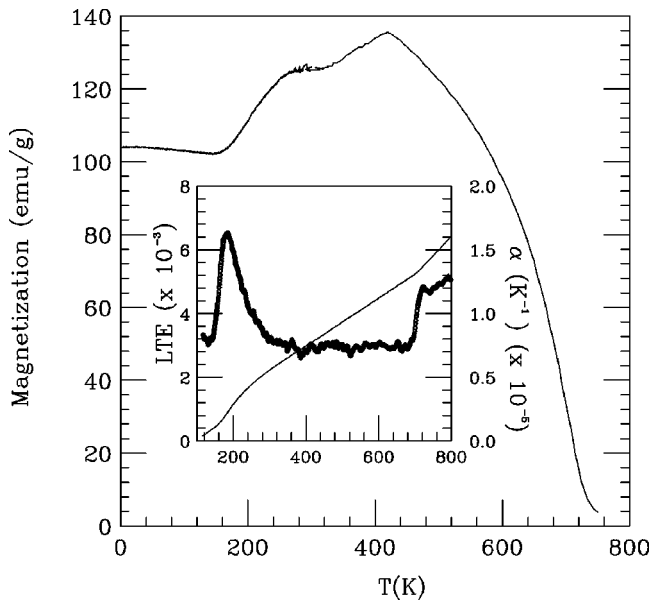


FIG. 1. Thermal dependence of the magnetization of $\text{Fe}_{0.51}\text{Rh}_{0.49}$ under an applied field of 6 kOe. In the inset linear thermal expansion (LTE) (solid line) and LTE coefficient (\circ) are shown.

the polarization rates from 97% down to about 11%, 5%, and 12% for Rh L_2 , Rh L_3 , and Pd L_3 edges, respectively.¹²

XMCD signals were obtained through the difference of x-ray-absorption near-edge structure (XANES) spectra recorded consecutively either by reversing the helicity of the incident beam or by flipping the magnetic field (~ 10 kOe) generated by a superconducting electromagnet and applied along the beam direction. Samples were mounted with the incident plane tilted 45° away from the beam direction and XANES spectra were recorded at different fixed temperatures in the fluorescent detection mode. The spin dependent absorption coefficient was obtained as the difference of the absorption coefficient $\mu_c = (\mu^- - \mu^+)$ for antiparallel μ^- and parallel μ^+ orientation of the photon helicity and the magnetic field applied to the sample. Spectra were normalized to the absorption coefficient at high energy to eliminate the dependence of the absorption on the sample thickness. The comparison of the spectra with those recorded in the transmission mode allows us to consider no correction for self-absorption effects.¹³

The thermal dependence of the magnetization of $\text{Fe}_{1.005}(\text{Rh}_{0.85}\text{Pd}_{0.15})_{0.995}$ shows all the hallmarks of the characteristic ferromagnetic (F)-antiferromagnetic (AF) phase transition of the FeRh alloys. As the temperature decreases it is observed an increase of the magnetization at $T_C = 590$ K. Near room temperature a sharp decrease of the magnetization occurs as a consequence of the F-AF, the magnetization becoming practically zero at room temperature under an applied magnetic field of 5 kOe.¹⁰ However, in the case of the $\text{Fe}_{0.51}\text{Rh}_{0.49}$ sample the behavior of magnetization is markedly different; see Fig. 1. The value of the magnetization at 4.2 K is $\sim 1.47\mu_B$ under a steady magnetic field of 6 kOe, and it remains nearly constant as temperature increases up to about 150 K. At this temperature (T_{FF}) the magnetization departs from the low-temperature constant regime and starts to increase continuously up to reach a value of $\sim 1.77\mu_B$ at room temperature. Linear thermal expansion

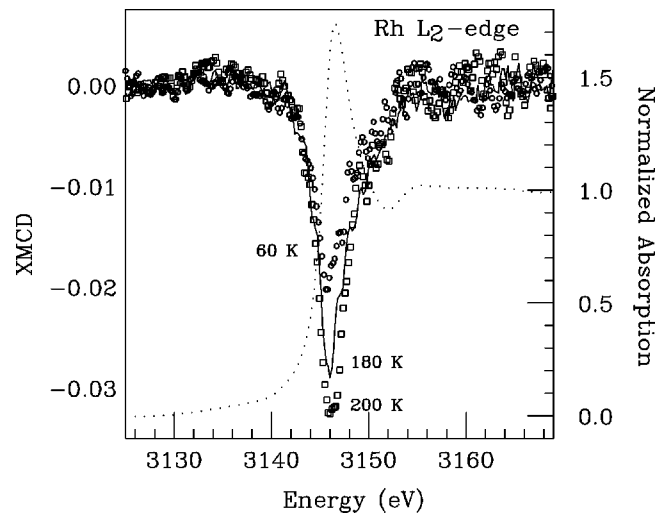


FIG. 2. Normalized Rh L_2 XMCD spectra of $\text{Fe}_{0.51}\text{Rh}_{0.49}$ recorded at different temperatures: $T = 60$ K (\circ), $T = 180$ K (solid line), and $T = 200$ K (\square). The spin averaged absorption recorded at 180 K is also shown (dots).

(LTE) measurements show a decrease of the LTE at T_{FF} and the thermal dependence of the LTE coefficient presents a pronounced anomaly at this temperature. Both effects indicate the appearance of magnetic transition at T_{FF} resembling the F-AF transition of the FeRh and $\text{Fe}_{1.005}(\text{Rh}_{0.85}\text{Pd}_{0.15})_{0.995}$. However, present results indicate that for the $\text{Fe}_{0.51}\text{Rh}_{0.49}$ composition the transition takes place between two F phases of different volume. As the cusp of the magnetization at ~ 400 K is due to an equiatomic FeRh impurity estimated to be less than the 8%, we have checked that this effect cannot be due to the presence of α' -FeRh phase. The temperature and field dependence of both magnetization and magnetostriction rule out this possibility.¹⁴

The magnetic behavior $\text{Fe}_{0.51}\text{Rh}_{0.49}$ showing this F-F transition is outstanding even as compared with the peculiar behavior of the Fe-Rh alloys. Indeed, $\text{Fe}_{0.51}\text{Rh}_{0.49}$ exhibits at the F-F transition all the hallmarks of anti-Invar effect, as previously reported for the F-AF transition of equiatomic FeRh (Ref. 3) in which the transition from the low to high volume phase has been interpreted in terms of the collapse of the Rh magnetic moment. Therefore, it is of primordial interest to determine the evolution of μ_{Rh} through this F-F transition. To this end, we have studied the XMCD at the Rh $L_{2,3}$ as a function of temperature. Selected XMCD signals obtained as a function of temperature as described above are reported in Fig. 2 for the Rh L_2 edge in the $\text{Fe}_{0.51}\text{Rh}_{0.49}$ sample. The shape and signs of the XMCD signals at both L_2 and L_3 edges do not vary either at the F-F transition or in all the temperature range studied. This result indicates that the coupling between Fe and Rh sublattices remains unaltered in both low and high volume phases. According to Brouder and Hikam¹⁵ the XMCD signals, defined as above, at the $L_{2,3}$ edges are proportional to the reduced transition probability towards spins parallel (antiparallel) to the net magnetization of the sample $\sigma^{\uparrow(\downarrow)}$ through the relations $\mu_c \alpha \sigma^{\uparrow} - \sigma^{\downarrow}$ and $\mu_c \alpha \sigma^{\downarrow} - \sigma^{\uparrow}$ for the L_2 and L_3 edges, respectively. The negative (positive) sign of the Rh XMCD signal at the L_2 edge (L_3) indicates that the Rh spin is antiparallel with respect to

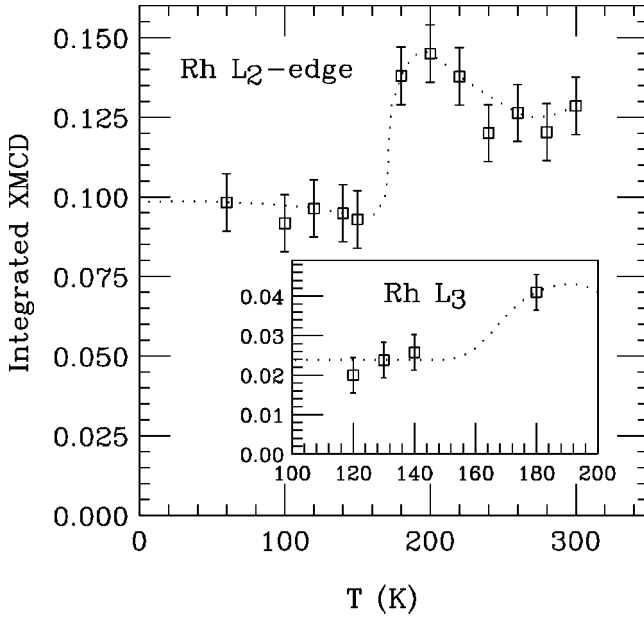


FIG. 3. Temperature dependence of the integrated XMCD signal at the Rh L_2 edge in the $\text{Fe}_{0.51}\text{Rh}_{0.49}$ compound. The inset reports the Rh L_3 integrated XMCD. (The dotted line is an eye guide.)

the magnetization direction in the material. Therefore, both Fe and Rh magnetic moments are parallel and ferromagnetically coupled in the two phases.

However, the existence of a non-negligible Rh XMCD signal below ~ 150 K excludes the collapse of the Rh magnetic moment in the low-temperature low volume phase. This is shown in Fig. 3 where the temperature dependence of the integrated XMCD signals is reported. There is a clear difference between the XMCD signals below and above $T = 150$ K, indicating the first-order nature of the F-F transition. Whereas in a characteristic FeRh F-AF transition, the complete collapse of the Rh moment takes place, our XMCD data support that μ_{Rh} stands, although reduced, in the low-temperature phase. This result is in agreement with the suggestion that this moment is induced by the exchange field at a rhodium atom from neighboring Fe moments by a polarization process.¹⁶ Indeed, the temperature dependence of the Rh $L_{2,3}$ absorption white lines shows that the intensity of the white line, linked to the localization of the Rh ($4d$) states,¹⁷ is higher and nearly constant for temperatures below 150 K than above the F-F transition. Therefore the Rh $4d$ states are more localized at low temperatures with a subsequent reduction of the Rh-Fe hybridization resulting in the depletion of the Rh magnetic moment. This result is supported by the temperature dependence of the Rh $L_{2,3}$ and Pd L_3 XMCD signals of $\text{Fe}_{1.005}(\text{Rh}_{0.85}\text{Pd}_{0.15})_{0.995}$. The sign of the XMCD indicates that not only Rh but also Pd atoms carry a non-negligible magnetic moment in the F phase, and that both μ_{Rh} and μ_{Pd} are ferromagnetically coupled to μ_{Fe} . The temperature dependence of the integrated XMCD signals through the F-AF transition is shown in Fig. 4. Both Rh and Pd signals follows the whole magnetization behavior in agreement with the hypothesis that these, μ_{Rh} and μ_{Pd} , magnetic moments arise from the exchange field at Rh and Pd atoms induced from neighboring Fe moments through a polarization process.

Finally, trying to obtain a deeper insight on the magnitude

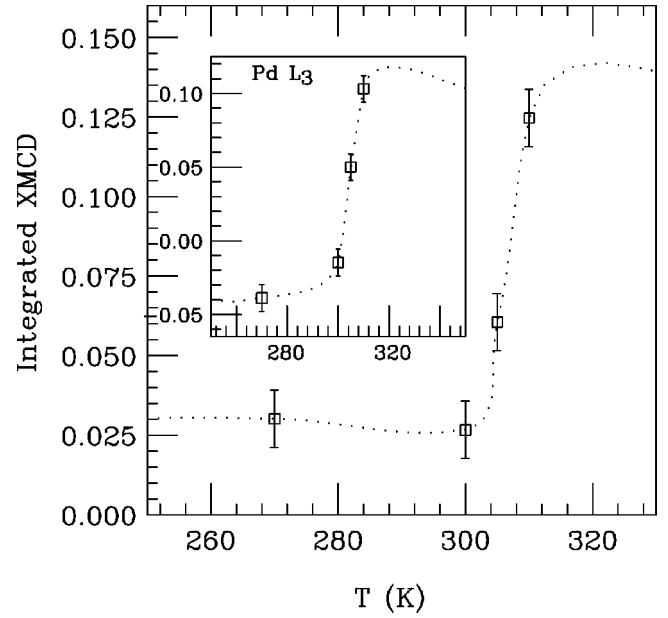


FIG. 4. Temperature dependence of the integrated XMCD signal at the Rh L_2 edge in $\text{Fe}_{1.005}(\text{Rh}_{0.85}\text{Pd}_{0.15})_{0.995}$. The inset reports the Pd L_3 integrated XMCD. (The dotted line is an eye guide.)

of μ_{Rh} in both ferromagnetic phases, we have applied the sum rules derived by Thole and Carra to the XMCD spectra (corrected for the rate of circular polarization).¹⁸ For the Rh $L_{2,3}$ edges they can be written as: $\langle L_z \rangle = 2(A_3 + A_2) \times (n_{4d} / \sigma_{tot})$ and $\langle S_z \rangle = 3/2(A_3 - 2A_2) \times (n_{4d} / \sigma_{tot}) - 7/2\langle T_z \rangle$. A_3 and A_2 are the integrals over the dichroic signal at the L_3 and L_2 edges, respectively, n_{4d} is the number of holes in the Rh $4d$ band and σ_{tot} is the unpolarized $2p \rightarrow 4d$ cross section. It should be noted that we have assumed $\langle T_z \rangle$ to be negligible in the spin sum rule as previously discussed by Vogel *et al.*²⁰ We have used two different ways to estimate (n_{4d} / σ_{tot}) : (i) we have deduced experimentally σ_{tot} as $3/2(\sigma^+ + \sigma^-)$ and fixed the number of $4d$ holes according to different Rh configurations ($4d^7 5s^2$ and $4d^8 5s^1$),¹⁹ and (ii) we have estimated n_{4d} / σ_{tot} from the experimental Rh $L_{2,3}$ spectra by subtracting Ag-foil $L_{2,3}$ spectra as proposed by Vogel *et al.*²⁰ Moreover, we have normalized the value of μ_{Rh} derived by applying the sum rules to the XMCD of $\text{Fe}_{1.005}(\text{Rh}_{0.85}\text{Pd}_{0.15})_{0.995}$ at 310 K, to the $0.9\mu_B$ value proposed for the F phase,^{9,10} and then applying this factor to the $\text{Fe}_{0.51}\text{Rh}_{0.49}$ XMCD data. The results are displayed in Table I. Both methods yield similar results when using the Rh $4d^7 5s^2$ configuration, being in agreement with neutron data. These results imply that the magnetic moment on Rh atoms decreases by about 30% in the low volume ferromagnetic as compared with high-temperature F phase. The depletion of μ_{Rh} in the low volume phase supports the hypothesis that this moment is induced by the exchange field at a rhodium atom arising from Fe neighbors. Indeed, combined XMCD and magnetization data yields a reduction of the iron magnetic moment from $\sim 2.5\mu_B$ to $\sim 2.2\mu_B$ when cooling down through the F-F transition. To this respect, it is important to note that the values of L_z/S_z deduced from XMCD (see Table I) exhibit an increase in the low-temperature phase. It implies a reduced quenching of the orbital moment by the crystal field, that is in agreement with

TABLE I. Values of μ_{Rh} derived from the XMCD spectra of $\text{Fe}_{0.51}\text{Rh}_{0.49}$ by considering two different atomic configurations for Rh (d^7, d^8); using Vogel's method (Ag); and normalizing the XMCD at 310 K of $\text{Fe}_{1.005}(\text{Rh}_{0.85}\text{Pd}_{0.15})_{0.995}$ to $0.9\mu_B$ (Nor) (see text for details).

$T(\text{K})$	(d^7)	(d^8)	(Ag)	(Nor)	L_z/S_z
180	1.13 ± 0.05	0.70 ± 0.05	1.03 ± 0.05	0.92	0.18 ± 0.02
140	0.77 ± 0.05	0.47 ± 0.05	0.70 ± 0.05	0.63	0.22 ± 0.02
130	0.76 ± 0.05	0.48 ± 0.05	0.66 ± 0.05	0.59	0.24 ± 0.02
120	0.77 ± 0.05	0.48 ± 0.05	0.69 ± 0.05	0.62	0.30 ± 0.02
310	1.04 ± 0.05	0.62 ± 0.05	1.00 ± 0.05	0.90	0.27 ± 0.03

observed localization of the Rh $4d$ states for temperatures below the F-F transition and the subsequent reduction of the $\text{Fe}(3d)\text{-Rh}(4d)$ hybridization.

Summarizing, we have demonstrated the induced nature of both μ_{Rh} and $\mu_{Pd}\text{Fe}_{1.005}(\text{Rh}_{0.85}\text{Pd}_{0.15})_{0.995}$. We have also shown that in $\text{Fe}_{0.51}\text{Rh}_{0.49}$ the characteristic ferromagnetic-

antiferromagnetic (F-AF) showed by FeRh alloys is replaced by a new transition between two different ferromagnetic phases at about 150 K. The Rh magnetic moment is found to vary, as a first order process, between both phases. Estimates of μ_{Rh} have been obtained from the analysis of the XMCD data at the Rh $L_{2,3}$ edges, showing its depletion from $1.03\mu_B$ in the high-temperature phase to 0.70 in the low-temperature one. The magnetic behavior of $\text{Fe}_{0.51}\text{Rh}_{0.49}$ at the F-F transition can be accounted in terms of the anti-Invar effect. Moreover, while in the case of the F-AF transition this effect is linked to the complete collapse of the Rh moment, in the present case it yields to a partial depletion of μ_{Rh} through the reduction of the iron exchange field due to the localization of the Rh $4d$ states and, therefore, the decrease of the $\text{Fe}(3d)\text{-Rh}(4d)$ hybridization for temperatures below the F-F transition.

This work was partially supported by Spanish DGICYT Grant Nos. MAT96-0448 and MAT96-0826 and by the LEA-MANES collaboration program. The experimental work at the European Synchrotron Radiation Facility has been performed with the approval of the ESRF Program Advisory Committee (Proposal HE-119).

-
- ¹M. Fallot, *Ann. Phys. (Paris)* **10**, 291 (1938); M. Fallot and R. Hocart, *Rev. Sci.* **77**, 498 (1939).
- ²V. L. Moruzzi and P. M. Marcus, *Phys. Rev. B* **46**, 2864 (1992); **48**, 16 106 (1993).
- ³M. R. Ibarra and P. A. Algarabel, *Phys. Rev. B* **50**, 4196 (1994).
- ⁴G. R. Harp, S. S. P. Parkin, W. L. O'Brien, and B. P. Tonner, *Phys. Rev. B* **51**, 12 037 (1995).
- ⁵G. Shirane, C. W. Chen, P. A. Flinn, and R. Nathans, *Phys. Rev.* **131**, 183 (1963).
- ⁶P. Tu, J. Heeger, J. S. Kouvel, and J. B. Comly, *J. Appl. Phys.* **40**, 1368 (1969).
- ⁷E. F. Bertaut, A. Delapalme, F. Fowat, G. Roult, F. de Bergevin, and R. Pauthenet, *J. Appl. Phys.* **33**, 1123 (1962).
- ⁸F. Bertaut, F. de Bergevin, and G. Roult, *C. R. Hebd. Seances Acad. Sci.* **256**, 1688 (1962).
- ⁹G. Shirane, C. W. Chen, P. A. Flinn, and R. Nathans, *J. Appl. Phys.* **33**, 1044 (1963).
- ¹⁰M. R. Ibarra, P. A. Algarabel, C. Marquina, Y. Otani, S. Yuasa, and H. Miyajima, *J. Magn. Magn. Mater.* **140-144**, 231 (1995).
- ¹¹J. Goulon, N. B. Brookes, C. Gauthier, J. Goedkoop, C. Goulon-Ginet, M. Hagelstein, and A. Rogalev, *Physica B* **208&209**, 199 (1995).
- ¹²D. Lefebvre, P. Saintavit, and C. Malgrange, *Rev. Sci. Instrum.* **65**, 2556 (1994).
- ¹³It should be also noted that the sum rules are still applicable on fluorescence yield spectra: M. van Veenetal, J. B. Goedkoop, and B. T. Thole, *Phys. Rev. Lett.* **77**, 1508 (1996).
- ¹⁴C. Marquina, M. R. Ibarra, P. A. Algarabel, A. Hernando, P. Crespo, P. Agudo, A. R. Yavari, and E. Navarro, *J. Appl. Phys.* **81**, 2315 (1997); P. A. Algarabel, C. Marquina, Z. Arnold, and M. R. Ibarra (private communication).
- ¹⁵C. Brouder and M. Hikam, *Phys. Rev. B* **43**, 3809 (1991).
- ¹⁶J. S. Kouvel, *J. Appl. Phys.* **37**, 1257 (1966).
- ¹⁷A. Bianconi, in *X-ray Absorption: Principles, Applications, Techniques of EXAFS, SEXAFS and XANES*, edited by D.C. Koningsberger and R. Prins (John Wiley & Sons, New York, 1988).
- ¹⁸B. T. Thole, P. Carra, F. Sette, and G. van der Laan, *Phys. Rev. Lett.* **68**, 1943 (1992); P. Carra, B. T. Thole, M. Altarelli, and X. Wang, *ibid.* **70**, 694 (1993).
- ¹⁹C. T. Chen, Y. U. Idzerda, H.-J. Lin, N. V. Smith, G. Meigs, E. Chaban, G. H. Ho, E. Pellegrin, and F. Sette, *Phys. Rev. Lett.* **75**, 152 (1995).
- ²⁰J. Vogel, A. Fontaine, V. Cros, F. Petroff, J. P. Kappler, G. Krill, A. Rogalev, and J. Goulon, *Phys. Rev. B* **55**, 3663 (1997).